

Supporting Information

Single transition metal atom embedded antimonene monolayers as efficient trifunctional electrocatalysts for HER, OER and ORR: A density functional theory study

Song Lu^a, Huong Lan Huynh^a, Fengliu Lou^b, Kun Guo^{c*}, Zhixin Yu^{a*}

^aDepartment of Energy and Petroleum Engineering, University of Stavanger, 4036 Stavanger, Norway

^bBeyond AS, Kanalsletta 2, 4033 Stavanger, Norway

^cInstitute of New Energy, School of Chemistry and Chemical Engineering, Shaoxing University, Shaoxing 312000, China

Computational methods

To investigate the stability of vacancy-defect in Sb monolayer, the formation energy (E_F) of vacancy was estimated by formula S1¹:

$$E_f(V_{Sb}) = E_{V-Sb} - n \times E_{Sb} \quad (S1)$$

where E_{V-Sb} , n and E_{Sb} are the total energy of defective Sb monolayer, the number of Sb atoms and energy of each Sb atom in a pristine Sb monolayer, respectively.

The binding energy (E_b) of TM atoms embedded in the defected Sb monolayer was calculated based on equation S2:

$$E_b = E_{TM-Sb} - E_{Sb} - E_{TM} \quad (S2)$$

where E_{TM-Sb} , E_{Sb} and E_{TM} denote the total energies of TM embedded Sb monolayer, defected Sb monolayer and TM atoms, respectively. With such a definition, a more negative value of E_b indicates better thermodynamic stability.

The cohesive energies of bulk metal materials (E_c) can be obtained by equation S3:

$$E_c = (E_{bulk} - n \times E_{TM})/n \quad (S3)$$

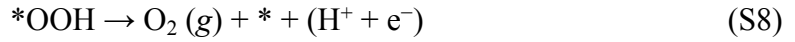
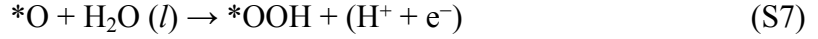
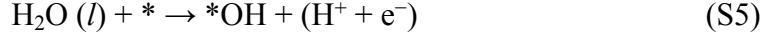
Where the E_{bulk} is the energies of bulk metal, E_{TM} is the energies of single metal atoms, and n is the number of metal atom in its bulk structure.

Besides, the formation energy of TM embedded in the defected Sb monolayer (E_f) was calculated as equation S4:

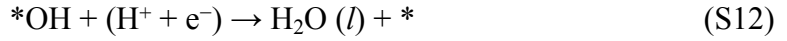
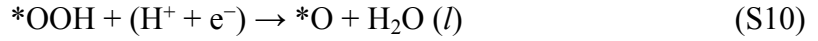
$$E_f = E_{TM-Sb} - \mu_{TM} - n\mu_{sb} \quad (S4)$$

where $E_{\text{TM-Sb}}$ is the energies of TM embedded in the defected Sb monolayer, n and μ_{sb} are the number of Sb atoms in defective Sb monolayer and the chemical potential of Sb from its bulk structure.

The detailed pathways of OER, ORR and HER have been summarized². In acidic condition, OER can be divided into the following four elementary steps S5-S9:



where $*$ denotes the substrates, l and g represent the liquid phase and gas phase. Whereas the ORR processes can be viewed as the opposite processes of OER, it can be represented by steps S9-S12:



The change of Gibbs free energy for the four elementary OER steps from ΔG_1 to ΔG_4 can be calculated as S16-S19:

$$\Delta G_1 = G(*OH) + G(\text{H}^+ + e^-) - G(\text{H}_2\text{O}) - G(*) \quad (\text{S16})$$

$$\Delta G_2 = G(*O) + G(\text{H}^+ + e^-) - G(*OH) \quad (\text{S17})$$

$$\Delta G_3 = G(*OOH) + G(\text{H}^+ + e^-) - G(*O) - G(\text{H}_2\text{O}) \quad (\text{S18})$$

$$\Delta G_4 = G(*) + G(\text{O}_2) + G(\text{H}^+ + e^-) - G(*OOH) \quad (\text{S19})$$

$$\text{and } G(\text{H}^+ + e^-) = G\left(\frac{1}{2}\text{H}_2\right) \quad (\text{S20})$$

Since DFT has poor description for the high-spin ground state of O_2 , the free energy of O_2 in the gas phase can be obtained by $G(\text{O}_2, g) + 2G(\text{H}_2, g) - 2G(\text{H}_2\text{O}, l) = 4.92$ eV. Meanwhile, it is difficult to directly get the free energy of H_2O in liquid phase, thus we calculated it from its vapor phase counterpart at their equilibrium pressure because of the same Gibbs free energy, which can be calculated by equation S21:

$$G(\text{H}_2\text{O}, l) = E_{\text{H}_2\text{O}} + \text{ZPE}_{\text{H}_2\text{O}} - \text{TS}_{\text{H}_2\text{O}} \quad (\text{S21})$$

where $E_{\text{H}_2\text{O}}$, $\text{ZPE}_{\text{H}_2\text{O}}$ and $\text{TS}_{\text{H}_2\text{O}}$ are the total energy of H_2O from DFT calculations in gas phase, zero-point energy and entropy respectively.

The changes of free energy in OER can be described as:

$$\Delta G_1 = G(*OH) \quad (\text{S22})$$

$$\Delta G_2 = G(*O) - G(*OH) \quad (S23)$$

$$\Delta G_3 = G(*OOH) - G(*O) \quad (S24)$$

$$\Delta G_4 = 4.92 - G(*OOH) \quad (S25)$$

Whereas the free energy changes in ORR processes from ΔG_a to ΔG_d can be expressed as below:

$$\Delta G_a = -\Delta G_4 \quad (S26)$$

$$\Delta G_b = -\Delta G_3 \quad (S27)$$

$$\Delta G_c = -\Delta G_2 \quad (S28)$$

$$\Delta G_d = -\Delta G_1 \quad (S29)$$

Therefore, the overpotential of OER and ORR can be evaluated from the following equations:

$$\eta_{\text{OER}} = \max \{ \Delta G_1, \Delta G_2, \Delta G_3, \Delta G_4 \} / e - 1.23 \quad (S30)$$

$$\eta_{\text{ORR}} = \max \{ \Delta G_a, \Delta G_b, \Delta G_c, \Delta G_d \} / e + 1.23 \quad (S31)$$

where 1.23 is the equilibrium potential.³

The HER under acidic conditions was also considered in this study, and the steps can be shown as below:



The HER activity was evaluated by calculating changes of the Gibbs free energy as in equation S34:

$$\Delta G_{*H} = \Delta E_H + \Delta ZPE - T\Delta S \quad (S34)$$

where ΔE_H is the adsorption energy of H_2 , ΔZPE and $T\Delta S$ are the differences of zero-point energy and entropy between the free H_2 and adsorbed H_2 . Using standard hydrogen electrode (SHE) as the energy reference, the closer the value of ΔG_{*H} to zero, the better HER performance of the catalysts, as shown by Nørskov et al.² Hydrogen adsorption should not be too weak or strong in HER, as typically shown in a volcano plot. The HER kinetics under equilibrium potential $U = 0$ and $pH = 0$ can be described by the theoretical exchange current i , according to the equation below:

$$i = -ek \frac{1}{1 + \exp\left(\frac{|\Delta G_H|}{k_b T}\right)} \quad (S35)$$

where k is the reaction rate constant, which was set to 1 under zero overpotential. k_b and T are the Boltzmann constant and temperature, respectively.

References

1. Q. X. Zhou, W. W. Ju, Y. L. Yong and X. H. Li, *J. Magn. Magn. Mater.*, 2019, **491**, 165613.
2. J. K. Nørskov, J. Rossmeisl, A. Logadottir, L. Lindqvist, J. R. Kitchin, T. Bligaard and H. Jónsson, *J. Phys. Chem. B*, 2004, **108**, 17886-17892
3. H. X. Xu, D. J. Cheng, D. P. Cao and X. C. Zeng, *Nat. Catal.*, 2018, **1**, 339-348.

Table S1. The calculated lattice constant a after structure relaxation with unit Å; the average bond length of $d_{\text{TM-Sb}}$ (the nearest three bonds) with unit Å. The binding energy E_b , cohesive energy E_c and formation energy E_f of TM@Sb monolayers with unit eV.

TM@Sb	a	$d_{\text{TM-Sb}}$	E_b	E_c	E_f
Sc	4.07	2.88	-8.47	-4.20	-3.85
Ti	4.09	2.76	-8.27	-5.47	-3.65
V	4.09	2.70	-7.44	-5.49	-2.83
Cr	4.09	2.69	-6.52	-3.78	-1.90
Mn	4.09	2.69	-6.73	-3.99	-2.11
Fe	4.09	2.59	-7.16	-5.11	-2.54
Co	4.06	2.45	-7.87	-4.94	-3.25
Ni	4.07	2.49	-8.02	-5.16	-3.40
Cu	4.08	2.56	-6.70	-3.84	-2.08
Zn	4.09	2.66	-4.98	-1.24	-0.36
Ru	4.09	2.56	-9.36	-7.25	-4.74
Rh	4.07	2.55	-9.61	-6.05	-5.00
Pd	4.09	2.61	-7.65	-3.70	-3.03
Ag	4.09	2.73	-5.92	-2.62	-1.30
Cd	4.10	2.83	-4.70	-0.89	-0.08
Ir	4.07	2.54	-10.34	-7.33	-5.73
Pt	4.08	2.59	-9.49	-5.53	-4.87
Au	4.11	2.67	-6.98	-3.08	-2.36
Pristine	4.11	2.89	-	-	-
V _{sb}	4.05	2.88	-	-	-1.77

Table S2. The calculated adsorption free energies of *H, *OH, *O and *OOH (ΔG_{*H} , ΔG_{*OH} , ΔG_{*O} and ΔG_{*OOH}), and each elementary step $\Delta G_{1/a}$, $\Delta G_{2/b}$, $\Delta G_{3/c}$, $\Delta G_{4/d}$ for OER and ORR (all units in eV); The overpotential of OER and ORR (η) for TM@Sb monolayers (all units in V).

Tm@Sb	ΔG_{*H}	ΔG_{*OH}	ΔG_{*O}	ΔG_{*OOH}	$\Delta G_{1/a}$		$\Delta G_{2/b}$		$\Delta G_{3/c}$		$\Delta G_{4/d}$		η	
					OER	ORR	OER	ORR	OER	ORR	OER	ORR	OER	ORR
Sc	0.63	-0.97	0.62	2.30	-0.97	-2.62	1.59	-1.68	1.68	-1.59	2.62	0.97	1.39	2.20
Ti	-0.28	-0.15	0.22	3.17	-0.15	-1.75	0.37	-2.95	2.95	-0.37	1.75	0.15	1.72	1.38
V	0.23	-1.54	-1.80	1.74	-1.54	-3.18	-0.26	-3.54	3.54	0.26	3.18	1.54	2.31	2.77
Cr	0.41	-0.71	-0.40	2.48	-0.71	-2.44	0.31	-2.88	2.88	-0.31	2.44	0.71	1.65	1.94
Mn	0.39	-0.55	-0.09	2.62	-0.55	-2.30	0.46	-2.71	2.71	-0.46	2.30	0.55	1.48	1.78
Fe	0.29	-0.58	-0.07	2.55	-0.58	-2.37	0.51	-2.62	2.62	-0.51	2.37	0.58	1.39	1.81
Co	0.25	-0.20	0.46	2.82	-0.20	-2.10	0.66	-2.36	2.36	-0.66	2.10	0.20	1.13	1.43
Ni	0.06	0.02	0.86	3.23	0.02	-1.69	0.84	-2.37	2.37	-0.84	1.69	-0.02	1.14	1.21
Cu	0.20	0.75	0.88	3.80	0.75	-1.12	0.13	-2.92	2.92	-0.13	1.12	-0.75	1.69	1.10
Zn	0.89	0.74	0.86	3.94	0.74	-0.98	0.12	-3.08	3.08	-0.12	0.98	-0.74	1.85	1.11
Ru	-0.37	-0.49	-0.09	2.42	-0.49	-2.50	0.40	-2.51	2.51	-0.40	2.50	0.49	1.28	1.72
Rh	0.40	0.67	1.30	3.72	0.67	-1.20	0.63	-2.42	2.42	-0.63	1.20	-0.67	1.18	0.60
Pd	0.22	0.65	1.66	3.78	0.65	-1.14	1.01	-2.12	2.12	-1.01	1.14	-0.65	0.89	0.58
Ag	0.39	0.73	1.47	4.04	0.73	-0.88	0.74	-2.57	2.57	-0.74	0.88	-0.73	1.34	0.50
Cd	0.98	0.70	1.31	4.27	0.70	-0.65	0.61	-2.96	2.96	-0.61	0.65	-0.70	1.73	0.62
Ir	-0.009	0.45	0.72	3.60	0.45	-1.32	0.27	-2.88	2.88	-0.27	1.32	-0.45	1.65	0.96
Pt	-0.01	0.52	1.90	3.61	0.52	-1.31	1.38	-1.71	1.71	-1.38	1.31	-0.52	0.48	0.71
Au	0.49	1.40	1.63	4.47	1.40	-0.45	0.23	-2.84	2.84	-0.23	0.45	-1.40	1.61	1.00
Pristine	1.34	1.45	1.97	4.56	1.45	-0.36	0.52	-2.59	2.59	-0.52	0.36	-1.45	1.36	0.87

Table S3. The calculated adsorption free energies of ΔG_{*H} for Ir@Sb monolayer with units in eV; The calculated adsorption free energies of ΔG_{*OH} , ΔG_{*O} and ΔG_{*OOH} , and $\Delta G_{1/a}$, $\Delta G_{2/b}$, $\Delta G_{3/c}$, $\Delta G_{4/d}$ for OER and ORR for each elementary step for Pt@ and Ag@Sb monolayers (all units in eV); The overpotentials of OER and ORR (η) for Pt@

U	Tm@Sb	ΔG_{*H}	ΔG_{*OH}	ΔG_{*O}	ΔG_{*OOH}	$\Delta G_{1/a}$		$\Delta G_{2/b}$		$\Delta G_{3/c}$		$\Delta G_{4/d}$		η	
						OER	ORR	OER	ORR	OER	ORR	OER	ORR	OER	ORR
2.5	Ir	-0.014	-	-	-	-	-	-	-	-	-	-	-	-	-
	Pt	-	0.53	1.93	3.65	0.53	-	1.40	-	1.71	-	1.28	-	0.49	-
	Ag	-	0.75	1.50	4.08	-	-0.84	-	-2.58	-	-0.75	-	-0.75	-	0.48
3.0	Ir	-0.010	-	-	-	-	-	-	-	-	-	-	-	-	-
	Pt	-	0.48	1.87	3.62	0.48	-	1.39	-	1.75	-	1.30	-	0.52	-
	Ag	-	0.74	1.52	4.05	-	-0.87	-	-2.53	-	-0.78	-	-0.74	-	0.49
3.5	Ir	-0.013	-	-	-	-	-	-	-	-	-	-	-	-	-
	Pt	-	0.52	1.90	3.64	0.52	-	1.38	-	1.74	-	1.28	-	0.51	-
	Ag	-	0.70	1.50	4.09	-	-0.83	-	-2.59	-	-0.80	-	-0.70	-	0.53

and Ag@Sb monolayers (unit in V). All calculations are under PBE+U level (U= 2.5, 3.0 and 3.5 eV).

Table S4. Adsorption free energies ΔG_{*H} under 1/25, 1/16 and 1/8 hydrogen coverage for Ir@Sb monolayer (unit in eV).

Hydrogen coverage	ΔG_{*H}
1/25	0.078
1/16 (this work)	-0.009
1/8	-0.070

Table S5. The sum of zero-point energy (ZPE) and entropic corrections (TS) of different intermediates adsorbed on catalysts under 298.15K. The *d* band center of TM@Sb monolayers.

Tm@Sb	ZPE+TS				<i>d</i> band center
	*OH	*O	*OOH	*H	
Sc	0.22	0.01	0.36	0.07	1.27
Ti	0.25	0.02	0.33	0.13	0.69
V	0.26	0.04	0.37	0.14	0.74
Cr	0.26	0.04	0.32	0.14	0.26
Mn	0.25	0.04	0.32	0.11	-1.18
Fe	0.28	0.02	0.28	0.12	-1.18
Co	0.27	0.03	0.31	0.15	-1.25
Ni	0.28	0.05	0.30	0.18	-1.34
Cu	0.29	0.04	0.32	0.17	-2.30
Zn	0.28	0.04	0.32	0.14	-6.53
Ru	0.28	0.04	0.31	0.18	-0.78
Rh	0.29	0.02	0.29	0.16	-1.21
Pd	0.26	0.01	0.34	0.17	-2.47
Ag	0.29	0.03	0.32	0.16	-3.93
Cd	0.29	0.03	0.31	0.19	-8.16
Ir	0.30	0.04	0.31	0.18	-1.07
Pt	0.29	0.01	0.30	0.18	-2.54
Au	0.29	0.02	0.30	0.16	-3.67
Pristine	0.28	0.01	0.32	0.17	-

Fig. S1. The vacancy formation energy at different defect concentrations.

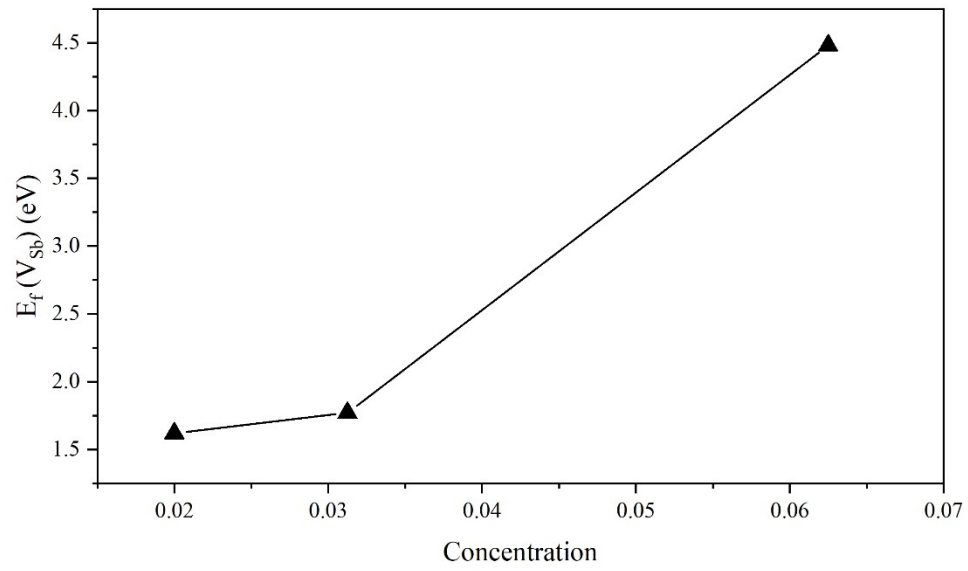


Fig. S2. The binding energy of Ir, Pt and Ag atoms with Sb monolayer at different concentrations for the SACs.

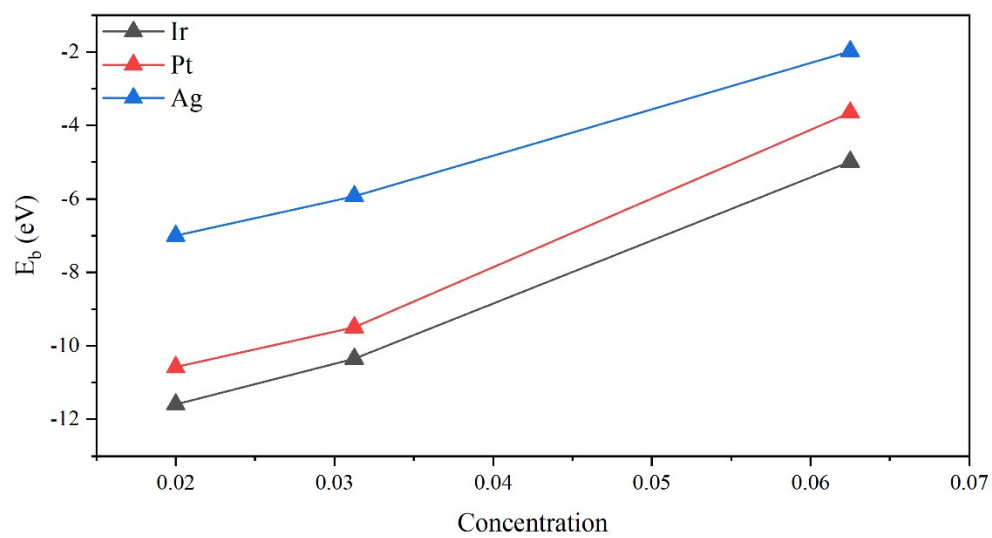


Fig. S3. The total density of states (DOS) of pristine Sb monolayer (a) and defective Sb monolayer (b); Fermi level was set to zero (dashed line).

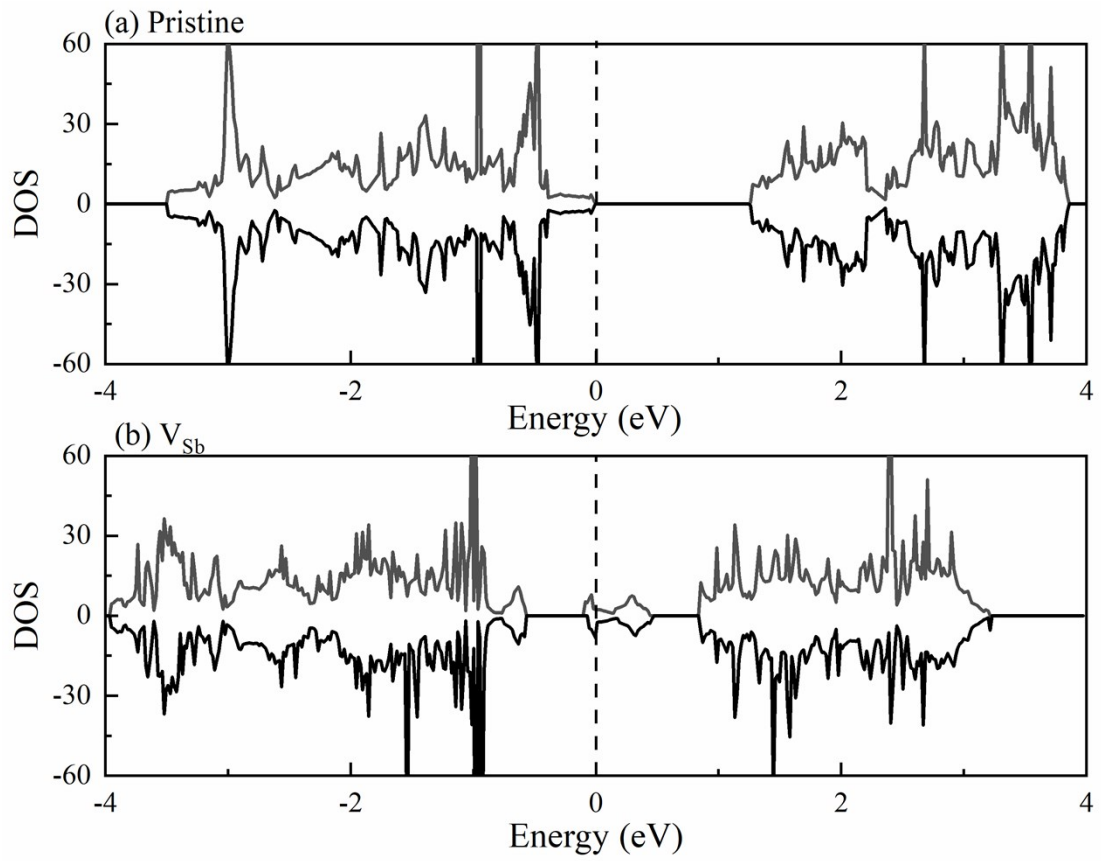


Fig. S4. The projected density of states of TM@Sb monolayers; Fermi level was set to zero (dashed line).

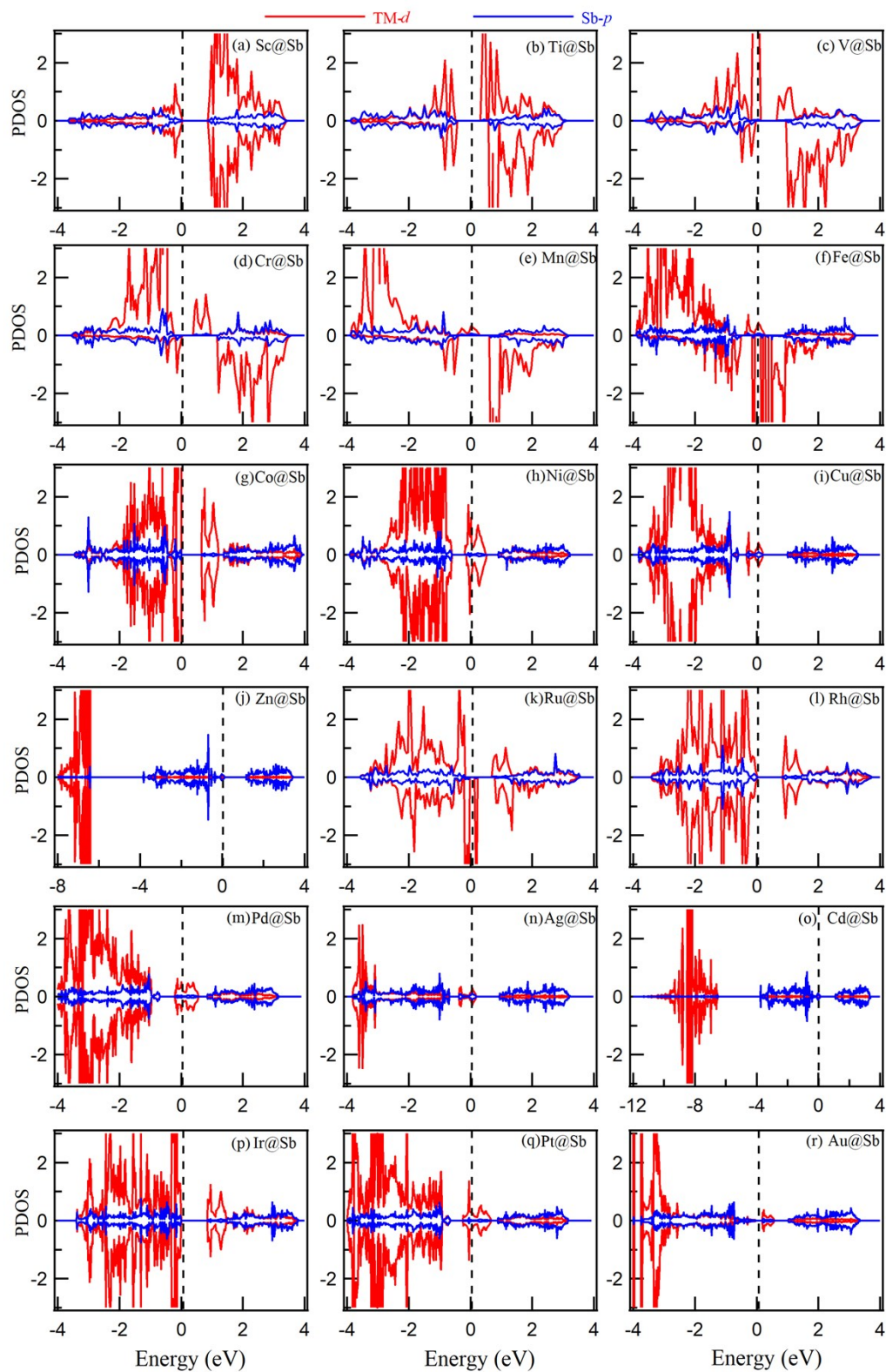


Fig. S5. The Gibbs free energy of hydrogen adsorption (ΔG_{*H}) for TM@Sb monolayers.

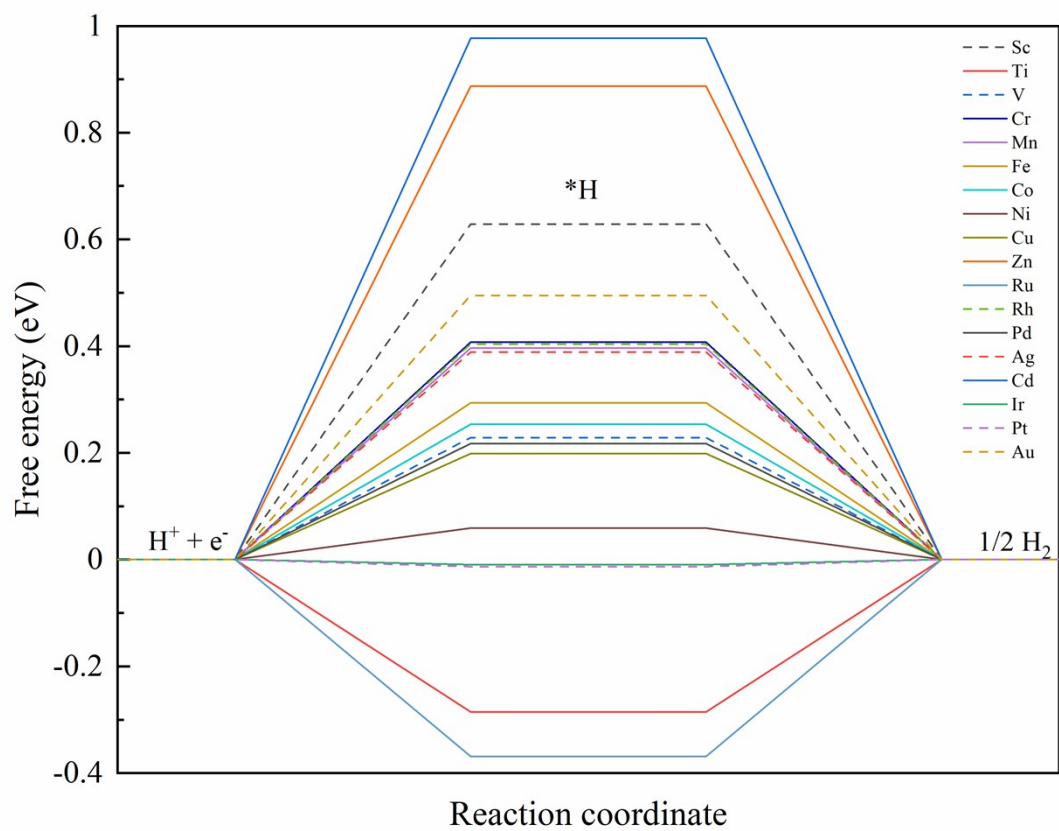
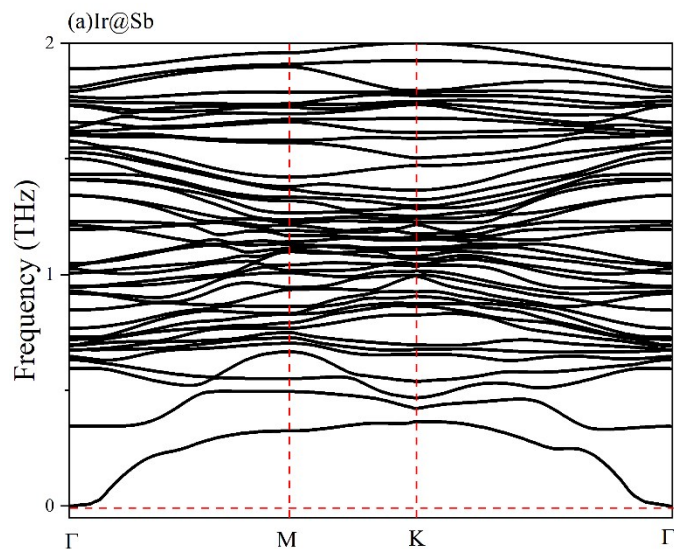


Fig. S6. (a) The phonon dispersion curves along the high symmetry directions; The total energy and structure variations of Ir@Sb monolayer at 300 K (b), 400 K (c), and 500 K (d) under AIMD simulation.



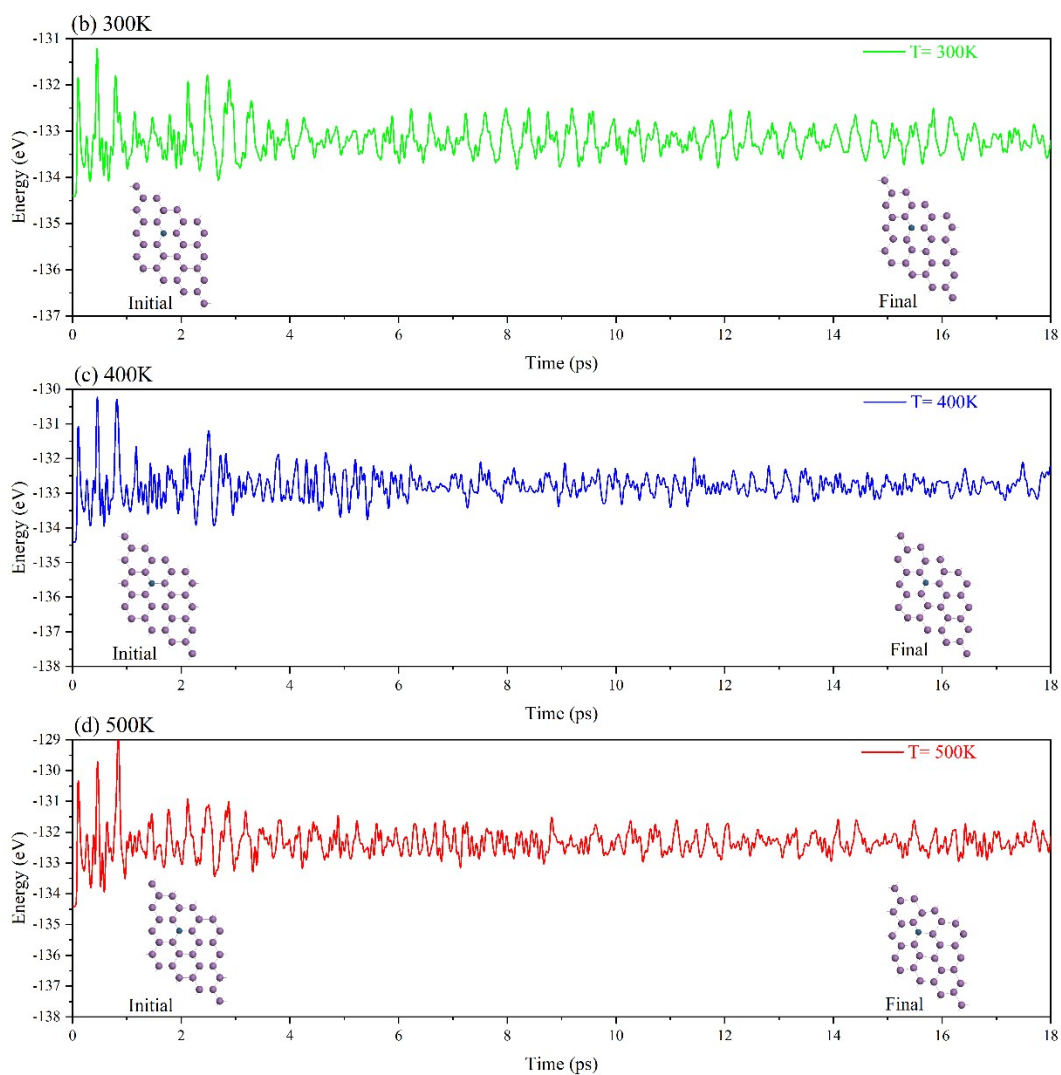


Fig. S7. The Gibbs free energy diagrams for OER/ORR elementary steps of TM@Sb monolayers (from Sc to Zn) under different potential.

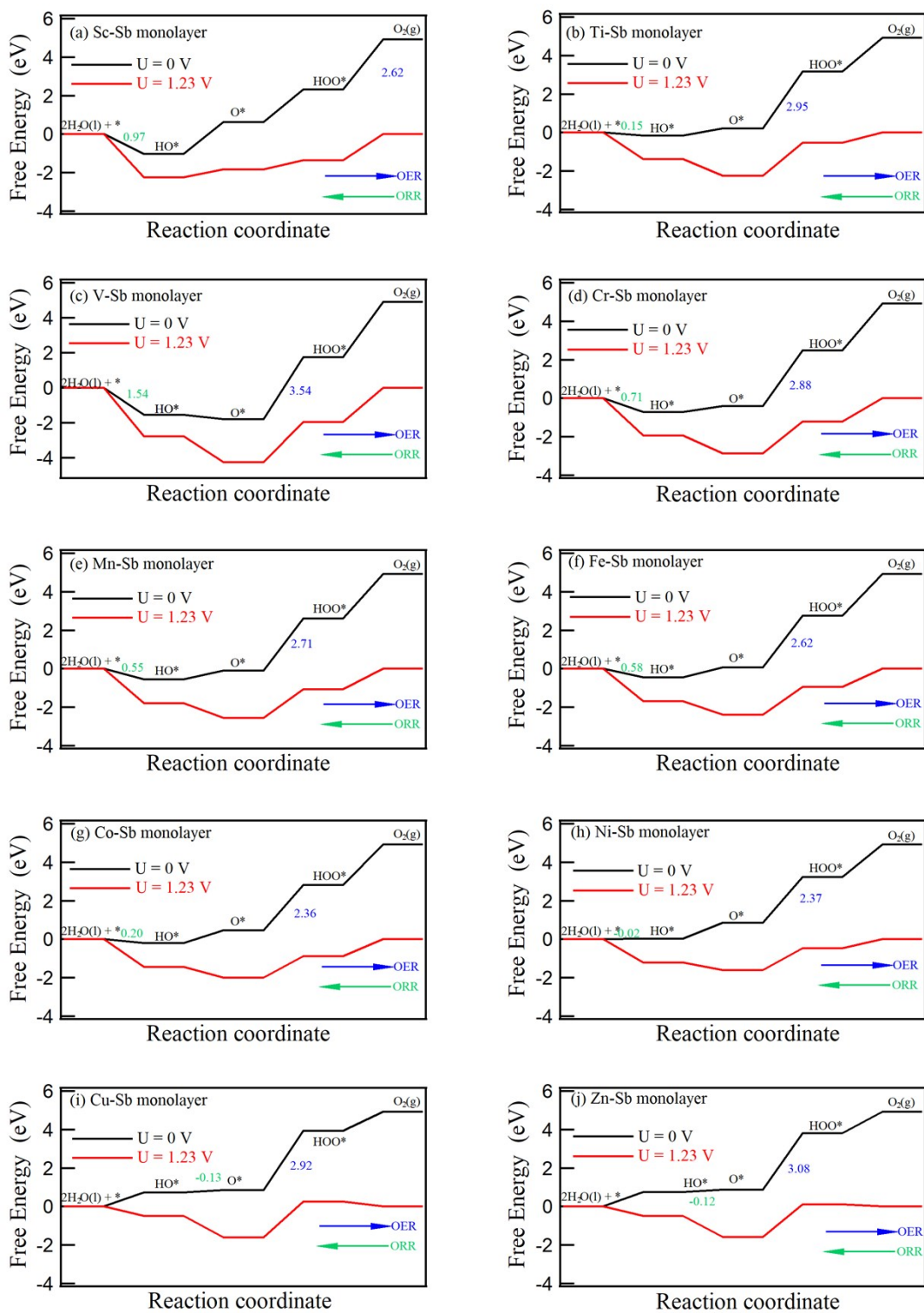


Fig. S8. The Gibbs free energy diagrams for OER/ORR elementary steps of TM@Sb monolayers (from Ru to Cd, and Ir to Au) under different potential.

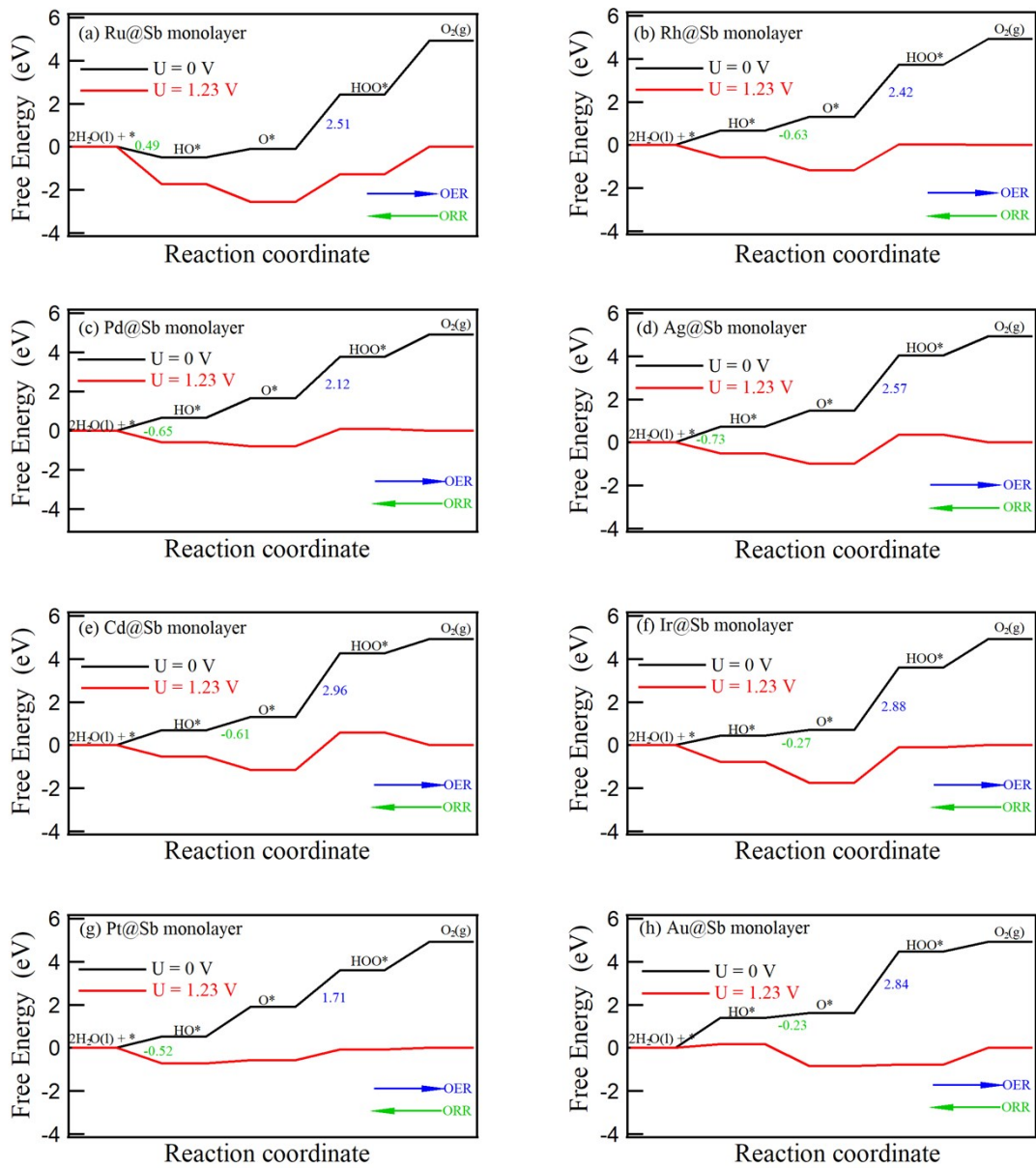


Fig. S9. (a) The phonon dispersion curves along the high symmetry directions; The total energy and structure variations of Pt@Sb monolayer at 300 K (b), 400 K (c), and 500 K (d) under AIMD simulation.

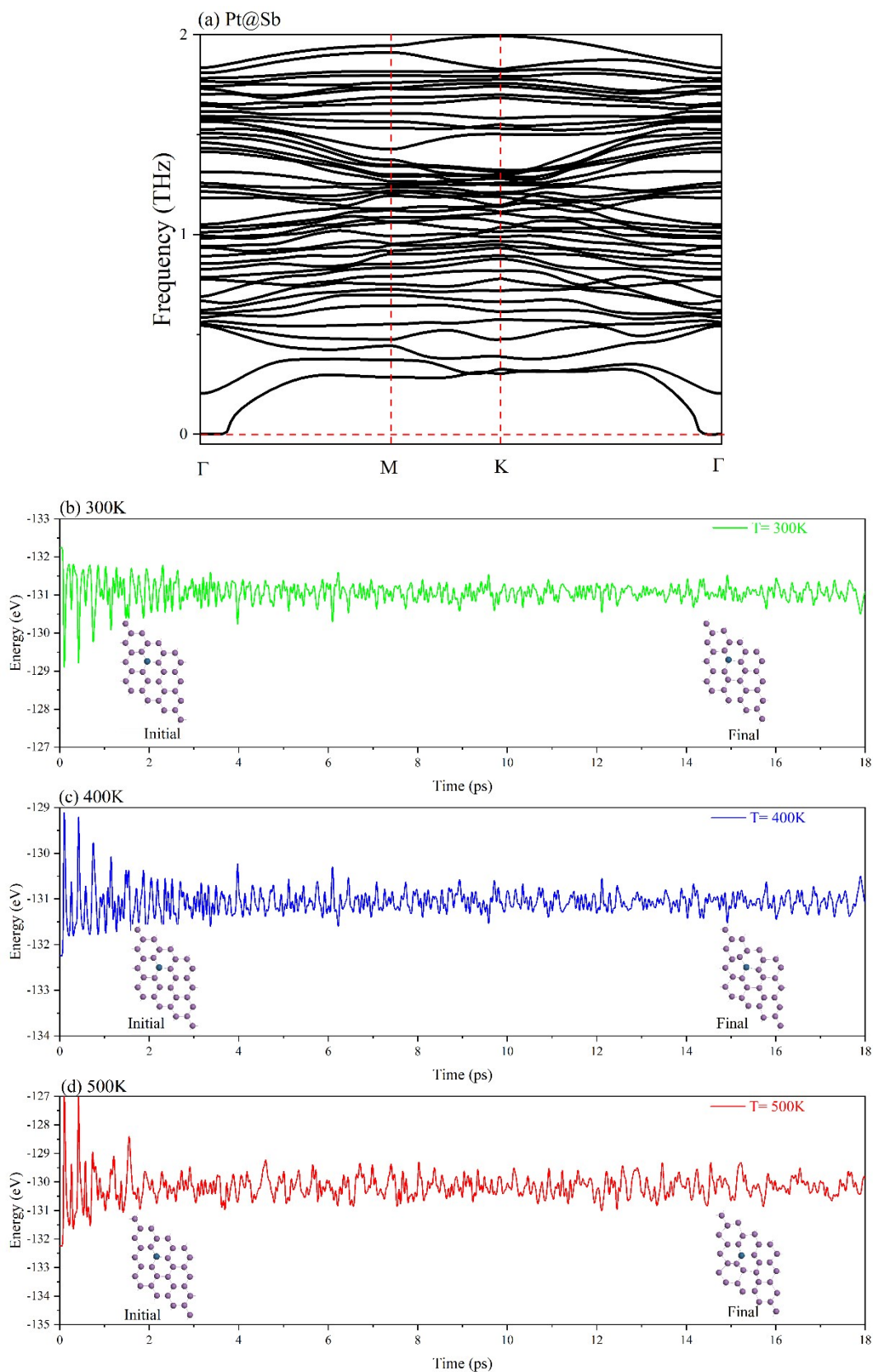


Fig. S10. (a) The phonon dispersion curves along the high symmetry directions; The total energy and structure variations of Ag@Sb monolayer at 300 K (b), 400 K (c), and 500 K (d) under AIMD simulation.

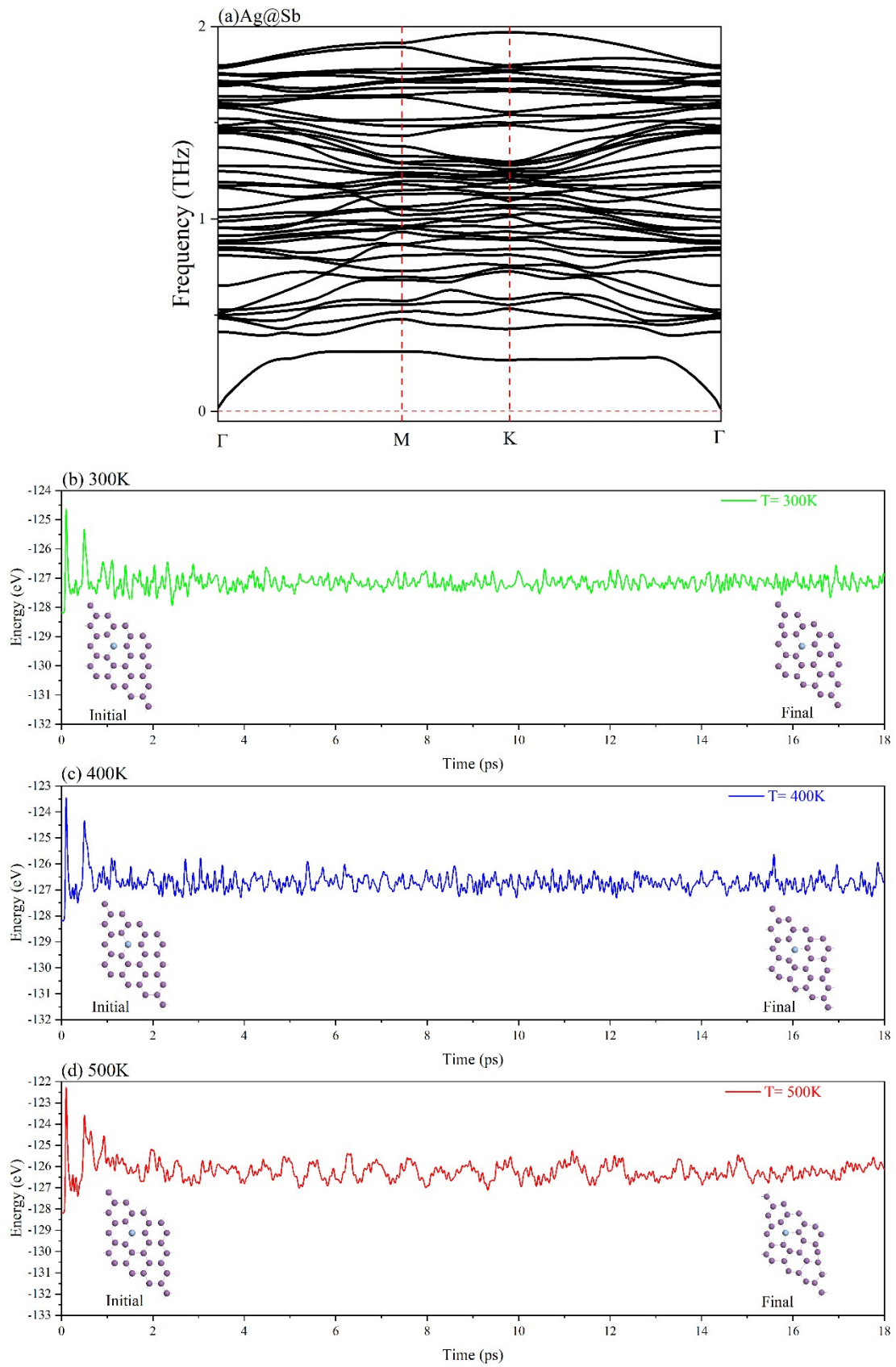


Fig. S11. The minimum energy pathway of adsorbed Pt atom diffused from the vacancy adsorption site to neighboring sites.

